

# Improved Design of a Dual Stator Winding Induction Generator for Wind Power Applications

Hossein Keshtkar  
Faculty of Engineering, Electrical Group  
Ferdowsi University of Mashhad  
Mashhad-IRAN  
[hkeshtkar@stu.um.ac.ir](mailto:hkeshtkar@stu.um.ac.ir)

Hossein Abootorabi Zarchi  
Faculty of Engineering, Electrical Group  
Ferdowsi University of Mashhad  
Mashhad-IRAN  
[abootorabi@um.ac.ir](mailto:abootorabi@um.ac.ir)

**Abstract**— In this paper, an optimized design of a dual stator winding induction generator (DWSIG) with standard squirrel cage rotor is proposed for wind turbine applications. Since the produced energy from the renewable energy usually is rather expensive thus, the efficiency criterion is suggested as the objective function. For a certain power, the DSWIG has a bigger core compared to the equivalent single-winding induction machine. In addition, the control winding frequency is three times bigger than power winding frequency. Therefore, the core losses minimization plays a significant role in machine efficiency improvement. In first step, the optimal parameter values are designed, and then the desired generator is evaluated through the finite-element method supported by Ansys Maxwell software. The obtained results verify a significant efficiency-optimized design of dual stator winding induction generator compared to conventional design.

**Keywords**- Genetic algorithms(GA); finite-element method(FEM); stator poles; rotor bars; dual stator winding induction generator .

## I. INTRODUCTION

During recent two decades, due to significant growth in the use of renewable energy, researchers have been attracted to research in this field. Wind energy is a renewable energy source with many inherent benefits. Initially the fixed speed wind turbines were presented due to advantages in simplicity, high reliability and low manufacturing cost and operation. However, the efficiency of these fixed speed turbines is low due to working at nearly constant speed, at the different wind speeds. To overcome this problem, variable speed wind turbines were designed to adjust the rotor speed for absorbing the maximum power possible in a certain range of the wind. Today doubly fed induction generator (DFIG) drives are the most common variable speed wind turbine systems. This configuration has a high efficiency and the inverter rating is typically 30% of total system power [1]. However, due to having a brush, the reliability is low and requires more maintenance. This issue is very important, especially for wind turbines installed at offshore areas. To solve the problems related to the brush, the concept of brushless dual stator winding induction generators was proposed. The brushless induction machines generally divided in two categories: dual stator winding induction machine (DSWIM) and brushless doubly fed induction machine (BDFIM). While the BDFIM

requires an expensive nested loops rotor design, the DSWIM commonly uses the standard squirrel-cage rotor design [2].

There are broadly two designs for DSWIM; the first type has two stator windings with dissimilar pole numbers and the second design has two stator windings wound for the same pole numbers. In the former case, because of the difference in the number of poles, dq equivalent circuit for both sets of stator windings are completely independent of each other and there is no coupling between the two windings. In this case for more utilize the magnetic material and avoid saturation and components harmonic elimination common between the two windings a ratio of 1: 3 between the poles of the machine is considered [3]. Due to the benefits of dissimilarity number of poles, the later method is used less.

In the last years, there have been published several papers related to the control and performance analysis of DWSIM [4]-[8]. However, not too many of them are related to the design and development of DWIGs with squirrel cage [9]-[11]. In [11], the DWIG has not been designed to optimize the efficiency.

In this paper, an optimal design of the DSWIG is presented for wind power application. In the first step, according to the efficiency criterion as selected objective function, the related parameters such as power and control winding number turns, current density, air-gap flux density magnitude and effective machine length are obtained and then, another objective function is selected in order to reduce the core losses compared to the initial design and other necessary design parameters such as dimensional parameters and magnetic values are determined using genetic algorithm. Finally, both of initially and optimized generators are investigated by simulation results in Ansys Maxwell software.

## II. OPTIMIZATION GENERATOR DSWIG METHOD

The machine operates in two modes, motoring and generating. Motoring mode is applied in electric vehicles and aerospace. Generating mode is used for wind power plants and small hydroelectric power. It should be noted that wind speed usually is variable and unstable. In order to get the maximum energy from the wind speed, wind energy systems must have the ability to adjust speed in the wide range. As mentioned in [5], one may notice that the equivalent circuit the machine is very interesting; since two windings have no any coupling. So the machine can be considered as two separate induction

machine coupled to each other through the rotor shaft. The reason why there is no coupling between the two sets of stator windings is dissimilarity in pole numbers. This difference should be more than one pair poles to avoid unbalanced tension on the rotor.

#### A. Optimization Algorithm Selection

The main criteria in optimized design of electrical machines are generally included: minimum computation required for the convergence of the algorithm, high accuracy of the obtained results and the lowest amount first and second derivatives in the process of the calculation algorithm. Almost all nonlinear optimization methods take a long time or dependent on first and second derivatives. However, among conventional methods, genetic algorithm approach has a high convergence to a global optimum, acceptable precision in calculations without first and second order derivatives. Therefore, in this paper, genetic algorithm (GA) is applied for optimization. The DWSIG optimization method is executed in order to determine optimization parameters include geometric, electrical and magnetic parameters in the equations related to objective function.

#### B. Design Process of DSWIG

As an objective function, the main goal is to increase the efficiency of the generator. But due to a lack of a reported standard or practical experiences about operating machine parameters is too hard to determine the upper and lower limits for some parameters such a efficiency and losses, regarding machine specification. So, the core loss minimization is considered such that the efficiency criterion exceeds an appropriate limit, while the convergence condition is satisfied.

The objective function is defined as:

$$\begin{cases} OF_1(x) = \eta^{k_1} \\ OF_2(x) = 1/P_{Core}^{k_2} \end{cases} \rightarrow OF(x) = OF_1(x) \times OF_2(x) = \eta^{k_1} / P_{Core}^{k_2} \quad (1)$$

Where  $x$  is optimization variable and  $K_i$  ( $i=1,2$ ) is zero or one, and thereby the definition of objective function changes; first,  $K_1$  is 1 and  $K_2$  is zero and vice versa. Then the optimal parameters are selected. The reason why we select the core losses as one of the components of the objective function is that the DSWIG air gap diameter is bigger than the conventional single winding induction machines with similar rating power. The definition and calculation method of objective function components are presented as follows.

A DSWIG is assumed with a 36/28 slot arrangement, 2:6 poles and 15 kW rated power which operates in synchronous mode. In this mode, the ratio of feeding frequencies of two stator winding is the same of the ratio of the number of poles. Here, power winding has a two-pole arrangement and 380 volt and 50 Hz which directly connected to the grid and control winding has a six-pole arrangement and 380 V and 150 Hz which is connected to the grid or DC supply by a three-phase inverter, as shown in Fig. 1.

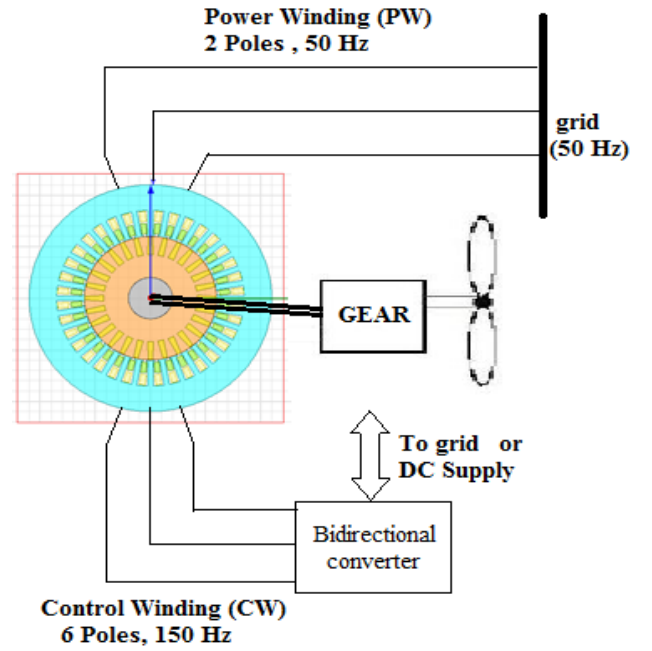


Fig 1. Operating system of DSWIG

#### 1) Efficiency Calculation

Efficiency in the DSWIG can be obtained as [9]:

$$\eta = \frac{P_{2/6}}{\left( \frac{\sqrt{2}\pi^2}{120} \right) K_w (D_{is}^2 L_e) \cos \phi \left[ n_{s2} B_{g2} K_{s2(rms)} + n_{s6} B_{g6} K_{s6(rms)} \right]} \quad (2)$$

In Eqn. (2),  $k_w$ ,  $D_{is}$  and  $L_e$  are winding factor, air gap diameter and machine effective length in millimeters, respectively and  $\cos \phi$  is machine power factor,  $n_{s2}$  and  $n_{s6}$  are synchronous speed field Power and control windings, respectively. Also,  $B_{g2}$  and  $B_{g6}$  are air gap peak flux densities for power and control windings,  $K_{s2(rms)}$  and  $K_{s6(rms)}$  respectively are surface current densities for power and control windings, respectively.

To calculate the  $B_g$  in DSWIG, we used the value of air gap flux density from an equivalent single-winding induction machine [12]. The number of poles equivalent single-winding induction machine is given as:

$$poles = \frac{P_P + P_C}{2} \quad (3)$$

Where  $P_P$  and  $P_C$  are the number of poles of power and control windings, respectively. Therefore a 15kW 4-pole induction machine fabricated by JEMCO Company with frame size 160L is selected [12]. The peak flux density for equivalent single-winding induction machine is in the range of 0.7 to 1 Tesla. Thus, using the equations of the air gap and stator yoke flux densities from both of DSWIG and equivalent machine, the peak values of air gap flux densities are estimated for power and control windings.

$$B_{g2} = 0.8975B_{g4} \quad (4)$$

$$B_{g6} = 0.2B_{g4} \quad (5)$$

Also the ratio between surface current density the power and control windings is calculated by [9]:

$$J_{(P/c)w} = \frac{6N_{(P/c)w}I_{(P/c)w}P_{(P/c)w}}{N_{ss}A_{S(P/c)}} \quad (6)$$

$$\begin{aligned} \frac{J_{Pw}}{J_{cw}} &= \frac{N_{Pw}I_{Pw}}{N_{cw}I_{cw}} \cdot \frac{p_{Pw}}{p_{cw}} \cdot \frac{d_{cw}}{d_{Pw}} \\ &= \frac{K_{s1}}{K_{s2}} \cdot \frac{p_{Pw}}{p_{cw}} \cdot \frac{d_{cw}}{d_{Pw}} \end{aligned} \quad (7)$$

In Eqns. (6) and (7),  $N_{Pw}$  and  $N_{cw}$  are the number of conductors per phase for power and control winding, and  $I_{Pw}$  and  $I_{cw}$  are phase current in conductors of power and control windings,  $p_{Pw}$  and  $p_{cw}$  are number of pole pairs of power and control windings, and  $A_{S(P/c)}$  is the conductors area of a slot in the power and control windings. Total surface current density of the power and control windings should be equal to surface current density of equivalent 4-pole single-winding induction machine which can be calculated easily [9].

## 2) Core Losses Calculation

Core losses are included eddy current and hysteresis losses. Eddy current loss for a sinusoidal flux density is proportional to the square of the maximum flux density in the core. The eddy current loss is equal to [14]-[15]:

$$P_{ec} = C_e \left\{ \begin{aligned} &N_{ss} \left[ f_p^2 (B_{P,max}^{ts})^2 + f_c^2 (B_{C,max}^{ts})^2 \right] v_{ts} \\ &+ N_{ss} \left[ f_p^2 (B_{P,max}^{cs})^2 + f_c^2 (B_{C,max}^{cs})^2 \right] v_{cs} \\ &+ N_r \left[ f_r^2 (B_{m,max}^{tr})^2 v_m^{tr} + f_r^2 (B_{m,max}^{cr})^2 v_m^{cr} \right] \end{aligned} \right\} \quad (8)$$

In Eqn. (8),  $C_e$  is a constant coefficient,  $N_{ss}$  and  $N_r$  are the stator and rotor number slots. Also,  $f_p$ ,  $f_c$  and  $f_r$  respectively are frequencies of power and control windings and frequency of rotor synchronous speed, and  $v_{(t,c)s}$  are the volume of tooth and yoke stator,  $B_{P(\setminus C),max}^{ts}$  and  $B_{P(\setminus C),max}^{cs}$  are peak flux densities of tooth and yoke stator of the power and control windings,  $B_{m,max}^{tr}$  and  $B_{m,max}^{cr}$  respectively are a peak flux density teeth and yoke rotor.

Various models for calculation of hysteresis loss were presented such as Jiles-Atherton, Preisach and Steinmetz that all of them need a practical laboratory setup to determine the coefficients and parameters in their equations. Steinmetz method is the most appropriate method with less computational volume and at least experimental parameters and acceptable accuracy [14], [16]. So, hysteresis loss is calculated for the machine as follows [15]-[16]:

$$P_{hys} = C_h \left\{ \begin{aligned} &N_{ss} f_p \left[ \left( f_{eq} (B^{ts}(t), f_p) \right)^{\alpha-1} (B_{max}^{ts})^\beta \right] v_{ts} \\ &+ N_{ss} f_c \left[ \left( f_{eq} (B^{cs}(t), f_c) \right)^{\alpha-1} (B_{max}^{cs})^\beta \right] v_{cs} \\ &+ N_r \left[ \begin{aligned} &f_r^\alpha (B_{max}^{tr})^\beta v_{max}^{tr} \\ &+ f_r^\alpha (B_{max}^{cr})^\beta v_{max}^{cr} \end{aligned} \right] \end{aligned} \right\} \quad (9)$$

Where in Eqn. (9),  $C_h$  is a constant coefficient,  $\alpha$  and  $\beta$  are power constants according to the type of material that the values are incorrect. The empirical values of  $\alpha$  and  $\beta$  are respectively in the range of 1 to 3 and 2 to 3 [16].

Equivalent frequency ( $f_{eq}$ ) of the stator which is calculated according to the rate of changes of magnetization is obtained as [14]:

$$f_{eq}(B(t), f) = \frac{2}{\pi^2 \Delta B^2} \int_0^T \left( \frac{dB}{dt} \right)^2 dt \quad (10)$$

In Eqn. (10),  $\Delta B$  is the peak to peak amplitude corresponding magnetic flux density.

The flux density values of Stator teeth and yoke and rotor can be calculated as follows [15].

$$B_{P(\setminus C),max}^{ts} = B_{P(\setminus C),max}^{ag} \frac{\pi D_{is} / N_{ss}}{2\pi / N_{ss} (0.5D_{ag} + h_{ss} / 3) - 0.5(b_{s1} + b_{s2})} \quad (11)$$

$$B_{P(\setminus C),max}^{cs} = B_{P(\setminus C),max}^{ag} \frac{\tau_{Pw(\setminus C)} (1.02 + 0.005 P_{P(\setminus C)})}{\pi h_{cs} k_{fe}} \quad (12)$$

$$B_{m,max}^{tr} = B_{m,avg}^{ag} \frac{D_{ag} - g}{k_{fe} [D_{ag} - g - 2h_r / 3 - b_{tr} / \alpha_{rs}]} \quad (13)$$

$$B_{m,max}^{cr} = B_{m,max}^{rt} \frac{\pi b_{tr}}{h_{cr}} \quad (14)$$

Geometric parameters of DSWIG are shown in Fig. 2. Control winding has a single-layer structure mounted on the bottom of the slot while power winding has a single-layer structure mounted on the top of the slot.

As shown in Table 1 and Table 2, the optimization variables and constrains were mentioned, respectively. Also, the tree diagram of generator design process is shown in Fig. 3. The proposed process can be used for designing other dual winding types.

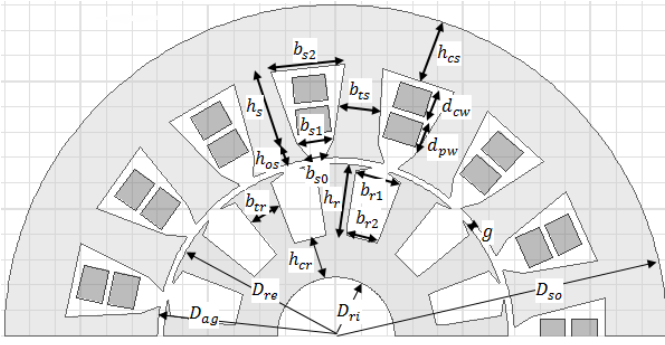


Fig. 2. Geometric structure of a dual stator winding induction generator

TABLE1. Design variables

Description	Parameter	Range
The average diameter of the air gap	$D_{ag} \sim x_1$	$150\text{mm} \leq x_1 \leq 300\text{mm}$
The axial length	$L_e \sim x_2$	$150\text{mm} \leq x_2 \leq 200\text{mm}$
Stator tooth width	$b_{ts} \sim x_3$	$5\text{mm} \leq x_3 \leq 10\text{mm}$
Stator slot height	$h_{ss} \sim x_4$	$20\text{mm} \leq x_4 \leq 28\text{mm}$
The thickness of the stator yoke	$h_{cs} \sim x_5$	$22\text{mm} \leq x_5 \leq 38\text{mm}$
The number of turns each phase power winding	$N_{pw} \sim x_6$	$18 \leq x_6 \leq 44$
The number of turns each phase control winding	$N_{cw} \sim x_7$	$24 \leq x_7 \leq 62$
Physical length of the air gap	$g \sim x_8$	$0.3\text{mm} \leq x_8 \leq 0.6\text{mm}$
Stretches angle of the rotor Slot	$\alpha_{rs} \sim x_9$	$8^\circ \leq x_9 \leq 12^\circ$
Rotor tooth width	$b_{tr} \sim x_{10}$	$5\text{mm} \leq x_{10} \leq 12\text{mm}$
Rotor slot height	$h_r \sim x_{11}$	$18\text{mm} \leq x_{11} \leq 30\text{mm}$
The thickness of rotor yoke	$h_{cr} \sim x_{12}$	$30\text{mm} \leq x_{12} \leq 45\text{mm}$
Current density power winding	$J_{pw} \sim x_{13}$	$5 \frac{\text{A}}{\text{mm}^2} \leq x_{13} \leq 7 \frac{\text{A}}{\text{mm}^2}$
Current density control winding	$J_{cw} \sim x_{14}$	$5 \frac{\text{A}}{\text{mm}^2} \leq x_{14} \leq 7 \frac{\text{A}}{\text{mm}^2}$
Air gap flux density	$B_{ag} \sim x_{15}$	$0.70\text{ T} \leq x_{15} \leq 1\text{ T}$

TABLE2. Design constrains

Description restrictions	Allowable range
Suitability slot and tooth width stator[13]	$0.3\tau_{ss} \leq \tau_{ss} - x_3 \leq 0.7\tau_{ss}$ $x_3 \geq 4\text{ mm}$
Suitability slot and tooth width rotor[13]	$0.3\tau_{sr} \leq \tau_{sr} - x_{10} \leq 0.7\tau_{sr}$ $x_{10} \geq 4\text{ mm}$
The minimum length physical air gap for IM [17]	$x_8 \geq \pi x_1 10^{-3} / P_p$
Suitability slot height of the stator and rotor	$2 \leq x_4 / b_{ts} \leq 5$ $2 \leq x_{11} / b_{tr} \leq 6$
The value of rotor current density constraint practical design machine[13]	$J_{rb} = I_r / x_{10} x_{11} \leq 6 \frac{\text{A}}{\text{mm}^2}$ $D_{so} / l_{fe} \leq 1.82$ $0.61 \leq D_{is} / D_{so} \leq 0.65$
flux density limits tooth and yoke stator [IEC60404-8]	1) $B_{ts} \leq 1.8\text{ T}$ , 2) $B_{cs} \leq 1.6\text{ T}$
flux density limits tooth and yoke rotor [IEC60404-8]	1) $B_{tr} \leq 2\text{ T}$ , 2) $B_{cr} \leq 1.7\text{ T}$

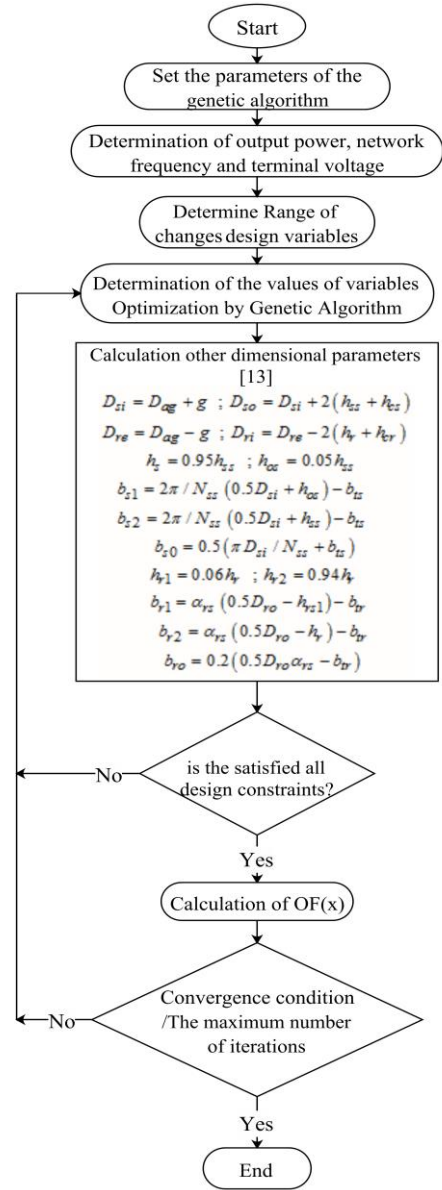


Fig. 3. A tree diagram process of generator design

### III. RESULTS OF OPTIMIZATION DESIGN IN ANSYS MAXWELL.16 SOFTWARE

In Table 3, the initial and optimized parameters related to the 15 kW prototype generator has been presented. The objective function is better for optimized structure compared to initial generator. Also in the optimal design, ratio of  $D_{ag} / l_{fe}$  is larger than an induction machine; because the machine has more pole numbers and poses a higher torque. By increasing the diameter of the air gap, there is the more space for the coils of power and control windings, thus the resistance of the coils of two windings reduces and the magnetizing inductance increase by reducing the saturation magnetic paths. Also, a significant improved efficiency occurs as the main goal of optimization. To evaluate the validity of the design process, the results of optimal design is compared with the

results of the finite element model. This comparison verifies the acceptable accuracy of the optimal design process.

TABLE3. Optimization results with data and specification prototype machine

Parameter	Initial design	Optimum design
$D_{ag}$	250 mm	232.9 mm
$L_e$	182.8 mm	195.7 mm
$b_{ts}$	8.5 mm	9.5 mm
$h_{ss}$	21.7 mm	25.2 mm
$h_{cs}$	34.6 mm	36.3 mm
$N_{pw}$	28	36
$N_{cw}$	44	56
$g$	0.45 mm	0.53 mm
$\alpha_{rs}$	10°	8.2°
$b_{tr}$	8 mm	10 mm
$h_r$	21.3 mm	23.8 mm
$h_{cr}$	32 mm	38.5 mm
$J_{pw}$	5.61 A/mm <sup>2</sup>	6.34 A/mm <sup>2</sup>
$J_{cw}$	4.69 A/mm <sup>2</sup>	5.31 A/mm <sup>2</sup>
$J_{rb}$	1.87 A/mm <sup>2</sup>	5.45 A/mm <sup>2</sup>
$B_{ag}$	0.8 T	0.78 T
$B_{ts}$	1.78 T	1.64 T
$B_{cs}$	1.53 T	1.38 T
$B_{tr}$	1.66 T	1.52 T
$B_{cr}$	1.33 T	1.21 T
$P_{Core}$	803.3 W	514.6 W
$\eta$	83.7%	91.3%
$OF(x)$	0.001041	0.001774

Also, in order to access a suitable design,  $D_{so} / l_{fe} \leq 1.82$  criterion is applied at final design to avoid Pancake design. Fig. 4 shows the lines of magnetic flux at designed generator in Ansys Maxwell software.

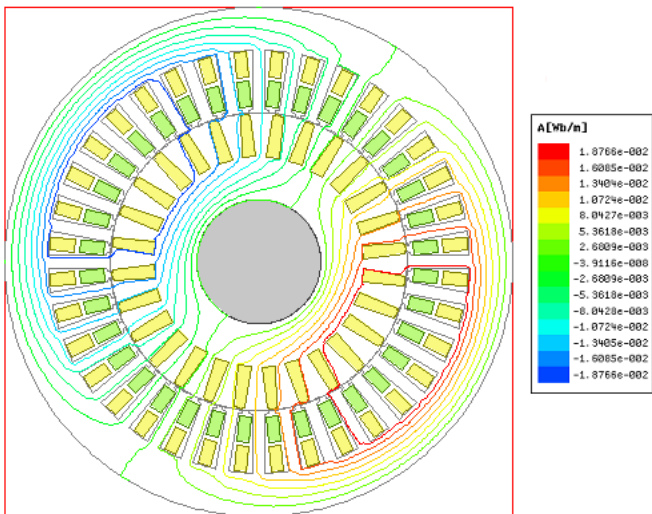


Fig. 4. Distribution of magnetic flux lines at designed generator

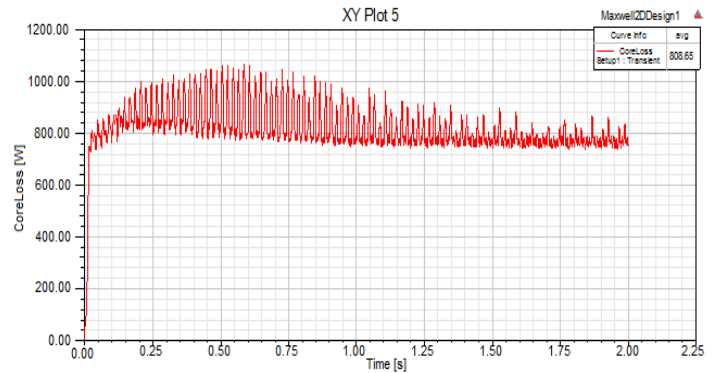


Fig. 5. Core losses before optimization

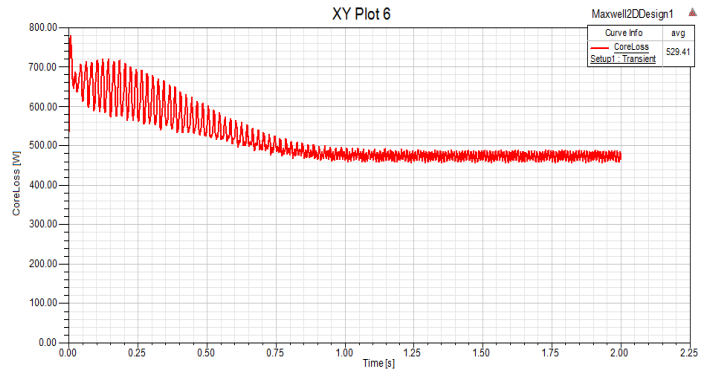


Fig. 6. Core losses after optimization

The results of the calculation of core losses in Ansys Maxwell before and after the design are shown in Figs. 5 and 6, respectively. As shown in these Figures, the core losses compared to non-optimized structure has improved about 35 percent. Consequently, this improvement plays a positive role on the main goal of optimization, efficiency, because the iron losses are specially the main component of losses in DSWG. Also, current waveforms in the power and control winding, induced voltage waveform in the power winding and electromagnetic torque waveform have been illustrated in Figs. 7-10.

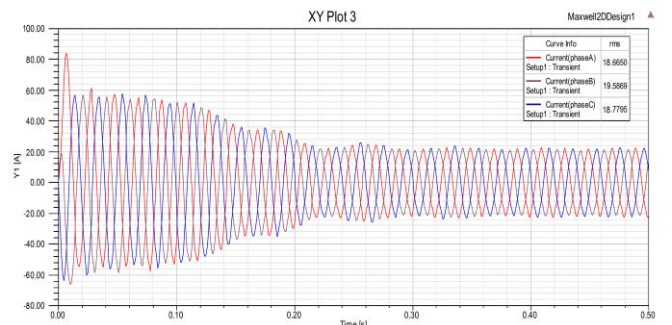


Fig 7. Power winding current

## REFERENCES

- [1] Frede Blaabjerg and Ke Ma, "Future on Power Electronics for Wind Turbine Systems," *IEEE Journal of Emerging and Selected Topics in Power Electronics*, vol.1, np. 3, September 2013.
- [2] S. Basak and C. Chakraborty, "Dual-stator-winding induction machine: Problems, progress, and future scope," *IEEE Trans. Ind. Electron.*, vol. 62, no. 7, pp.4641 -4652, 2015.
- [3] O. Ojo and Z. Wu, "Modeling of a dual-stator-winding induction machine including the effect of main flux linkage magnetic saturation," *IEEE Trans. Ind. Appl.*, vol.44, no.4, pp. 1099–1107, Jul./Aug. 2008.
- [4] F. Bu, Y. Hu, W. Huang, S. Zhuang, and K. Shi, "Wide-speed-range-operation dual stator winding induction generator DC generating system for wind power applications," *IEEE Trans. Power Electron.*, vol. 30, no. 2, pp. 561–573, Feb. 2015.
- [5] A. R. Muñoz and T. A. Lipo, "Dual stator winding induction machine drive," *IEEE Trans. Ind. Appl.*, vol. 36, no. 5, pp. 1369–1379, Sep./Oct. 2000.
- [6] R. Bojoi, F. Farina, G. Griva, and F. Profumo, "Direct torque control for dual three-phase induction motor drives," *IEEE Trans. Ind. Appl.*, vol. 41, no. 6, pp. 1627–1636, Nov./Dec. 2005.
- [7] R. N. Andriamalala, H. Razik, L. Baghli, and F.-M. Sargos, "Eccentricity fault diagnosis of a dual-stator winding induction machine drive considering the slotting effects," *IEEE Trans. Ind. Electron.*, vol. 55, no. 12, pp. 4238–4251, Dec. 2008.
- [8] Y. Li, Y. Hu, W. Huang, L. Liu, and Y. Zhang, "The capacity optimization for the static excitation controller of the dual-stator-winding induction generator operating in a wide speed range," *IEEE Trans. Ind. Electron.*, vol. 56, no. 2, pp. 530–541, Feb. 2009.
- [9] Z. Wu, "An investigation of dual stator winding induction machines", Thesis, Tennessee Technological University, USA, 2008.
- [10] L. Lingshun, Zhangkai and H. Yuwen, "Research on dual statorwinding induction generator with wind energy", *International Conference on Energy and Environment Technology*, vol. 1, pp. 790 – 793, 2009.
- [11] J. A. Barrado Rodrigo, X. Munte, H. Valderrama-Blavi, F. Gonzalez-Molina, "Design and testing of a dual stator winding induction generator", 2013 10th International Multi-Conference on Systems, Signals and Devices, SSD 2013.
- [12] <http://www.jemcomotor.ir/en/>
- [13] I. Boldea and S.A. Nasar, *The induction machine handbook*. CRC Press, 2002.
- [14] J. G. Zhu, and V. S. Ramsden, "Improved Formulations for Rotational Core Losses in Rotating Electrical Machines," *IEEE Tran. Magn.*, vol. 34, no. 4, pp. 2234-2242, Jul 1998.
- [15] H. Gorginpour, H. Oraee, and E. Abdi, "Calculation of core and stray load losses in brushless doubly fed induction generators," *IEEE Trans. Ind. Electron.*, vol. 61, no. 7, pp.3167–3177, Jul. 2014.
- [16] J. Reinert, A. Brockmeyer, and R. W. A. A. De Doncker, "Calculation of losses in ferro- and ferrimagnetic materials based on the modified Steinmetz equation," *IEEE Trans. Ind. Appl.*, vol. 37, no. 4, pp. 1055–1061, Jul. 2001.
- [17] Y. Duan and R. G. Harley, "A novel method for multiobjective design and optimization of three phase induction machines," *IEEE Trans. Ind. Appl.*, vol. 47, no. 4, pp. 1707–1715, Jul./Aug. 2011.

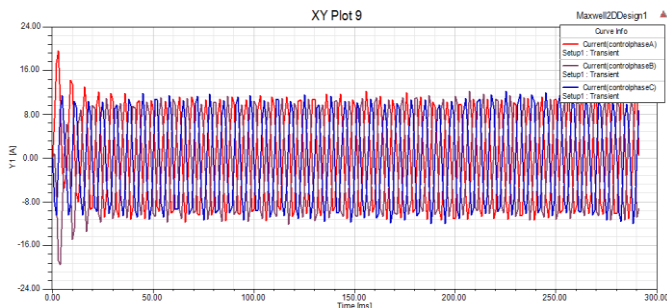


Fig 8. Control winding current

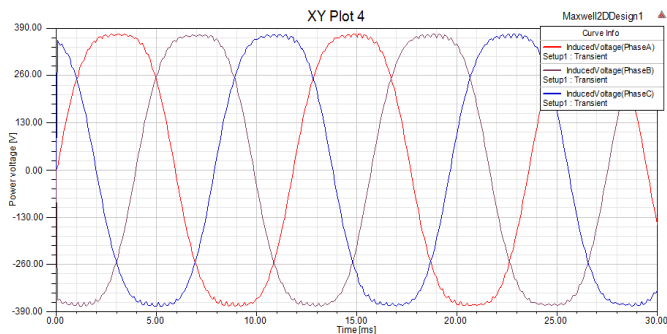


Fig 9. Power winding induced voltage

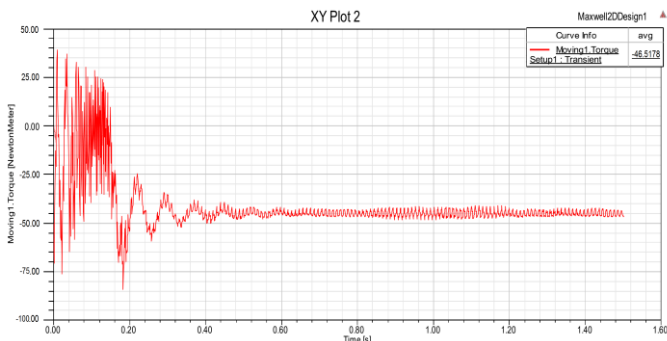


Fig 10. Electromagnetic torque waveform from a DSWIG

## IV. CONCLUSION

An optimization design flowchart based on genetic algorithm was presented for DSWIG with standard squirrel cage rotor to reduce core losses and as a result increases the overall efficiency. The obtained simulation results in Ansys Maxwell software verified the effectiveness and performance of proposed method. The core losses compared to non-optimized structure has reduced about 35 percent.